PAPER
Răzvan C. Cioc, Pieter C. A. Bruijnincx *et al.*
Efficient synthesis of fully renewable, furfural-derived building blocks *via* formal Diels–Alder cycloaddition of atypical addends

Check for updates

Efficient synthesis of fully renewable, furfural-derived building blocks *via* formal Diels–Alder cycloaddition of atypical addends†

Răzvan C. Cioc,*‡[a] Eva Harsevoort,‡[a] Martin Lutz[b] and Pieter C. A. Bruijnincx [iD] *[a]

Diels–Alder (DA) cycloaddition of furanics is emerging as a key transformation in circular chemistry, providing access to highly versatile, biobased platform molecules. Further development of this technology into viable industrial applications faces major challenges, a notorious one being the lack of reactivity of the most readily available furans, *i.e.* the furfural derivatives. Herein we describe the remarkably-facile intramolecular DA reaction of allyl acetals of different furfurals to efficiently afford formal DA adducts with the atypical, unreactive dienophile allyl alcohol. Our methodology gives access to unprecedented oxanorbornene derivatives in high chemo-, regio- and stereoselectivity, which can be readily diversified into valuable products. This offers the potential of scalable production of renewable chemical building blocks from cheap, bioderived platform molecules.

Introduction

Circularity and sustainability considerations require routes to be developed to produce 'drop-in' chemical commodities as well as novel, functional alternatives from renewable resources rather than fossil feedstock. For this, the Diels–Alder [4 + 2] cycloaddition (DA) of biobased furanics has emerged as a particularly useful synthetic tool,[1] as it allows fully atom-efficient conversion of bioderived feedstocks into highly useful products (*i.e.* bearing the ubiquitous 6-membered carbocyclic motif). Indeed, in addition to the usual synthetic targets of the century-old DA chemistry (natural products,[2–4] bioactive compounds,[5] drug delivery systems and biomaterials,[6,7] responsive polymers,[8–10] *etc.*), furan DA chemistry is now increasingly part of synthesis routes towards various renewable commodity and specialty chemicals, for potential application as (novel) monomers, adhesives, curing agents, plasticizers, lubricants, coatings, *etc.*[1,11–17]

To ensure both overall sustainability and economic viability, such furan DA conversion technology needs to be green

[a]*Organic Chemistry and Catalysis, Institute for Sustainable and Circular Chemistry, Faculty of Science, Utrecht University, Universiteitsweg 99, 3584 CG Utrecht, The Netherlands. E-mail: p.c.a.bruijnincx@uu.nl, r.c.cioc@uu.nl*
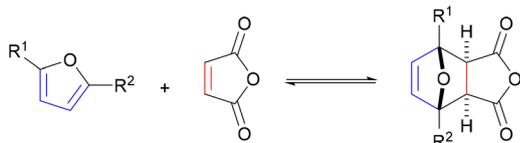[b]*Dr M. Lutz, Structural Biochemistry, Bijvoet Centre for Biomolecular Research, Faculty of Science, Utrecht University, Universiteitsweg 99, 3584 CG Utrecht, The Netherlands*

‡Equal first authorship contribution.

and efficient and based on the most readily available biobased furanics to ensure the necessary redox- and atom-efficiency. Meeting these prerequisites in full is a challenge. First of all, there is an unfortunate mismatch between those furans most directly accessible by biorefining and currently most abundantly produced and their DA reactivity: formyl-furans (furfural and derivatives) are essentially unreactive dienes.[18–21] Furthermore, the reactive dienophiles of choice, *e.g.* maleic anhydride (and derivatives thereof), are only available from biomass at max 80% theoretical carbon yield, impacting the carbon footprint of the process (Fig. 1B).[22] Indeed, the current scope of furan DA reactions is dominated by the so-called 'normal electron demand' cycloadditions of electron-rich furans and electron-deficient dienophiles, both activated inputs;[1,12] very few examples with alternative substitution patterns of the addends are available in the literature.[18,23] More so, adducts originating from the combination of electronically-mismatched pairs (*i.e.* electron-poor furan/electron-rich dienophile, both deactivated inputs) are absent altogether; this area of the oxanorbornene chemical space is essentially empty. Next, furan DA cycloadditions are typically equilibrium-limited, disallowing high product yields. In addition, the adduct is typically thermally labile, which limits the options and operating window for downstream processing. Finally, controlling the regiochemistry (and sometimes stereochemistry) of unsymmetrical addend coupling is highly challenging, as is the subsequent purification of the major isomer from the resulting mixture.[24]

Herein we report a novel strategy that addresses all these issues and enables the direct, selective and efficient pro-

A. Prototypical furan DA reaction: activated addends

R^1, R^2, mainly H, Me, CH_2OR
(and more recently $CH(OR)_2$)

R^1 = CHO, COR, COOR typically not tolerated
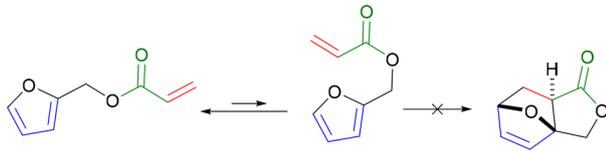(such MA adducts not reported in the literature)

- NED cycloaddition: activated addends
  i.e. electron-rich furan, electron-deficient dienophile

x oxanorbornenes with alternative substitution patterns are rare in literature
x regioselectivity control challenging in unsymmetrical systems
x inefficient sourcing of addends from biomass
x equilibrium reactions, often conversion is thermodynamically limited
x thermally-labile adducts, limited options for downstream chemistry

B. Processing of furfural into suitable inputs for the DA reaction

by catalytic hydrogenation
requires 2 equiv H_2

by catalytic oxidation
C atoms wasted as CO_2
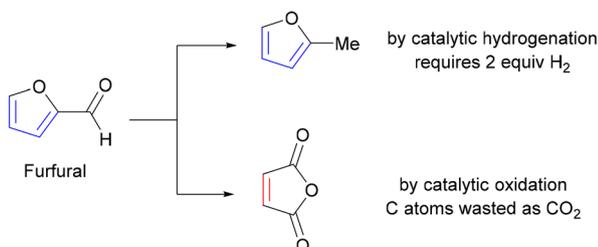
C. Prior work: intramolecular DA reaction of furfuryl acrylate failed

D. This work: facile intramolecular DA cycloaddition of furfural allyl acetals

recycle of regenerated allyl alcohol
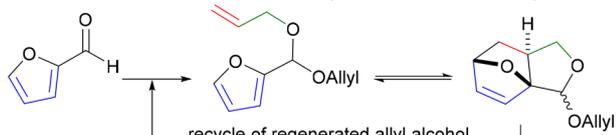
- Atypical diene/dienophile pair:
  i.e. electron-poor furan, electron-rich dienophile

✓ high chemo- and stereoselectivity; exclusive *ortho* regioselectivity
✓ convenient bioderived feedstocks, 100% C yield from biomass
✓ facile purification, scalable, versatile synthon as product
  (incl. towards <u>atypical</u> <u>adducts</u>)

**Fig. 1** Furan DA cycloaddition: current paradigm and design of novel route to new scaffolds.

duction of versatile DA adducts of furfural by exploiting an atypical dienophile, allyl alcohol. As part of our prior work on sustainable furan DA chemistry, we noted that the intramolecular DA cycloaddition with the bifunctional furfuryl acrylate[25] failed due to a highly unfavorable equilibrium between the most stable conformation of this molecule (*i.e.* linear) and

the necessary, reactive conformer (folded), originating among other factors from the large dipole moment of the latter. As intramolecular DA cycloaddition does offer the potential to overcome most of the challenges noted above, we did pursue this approach further and hypothesized that tethering the dienophile to the furan *via* an ether linkage instead would improve the conformational flexibility and thus allow the DA reaction. However, since the olefinic bond would no longer be electronically-activated, we anticipated a more difficult internal cycloaddition. Intramolecular furan DA reactions are fairly common and, encouragingly, have been reported for both activated as well as unactivated tethered dienophiles (mainly amine-based, but also (thio)ether or alkyl linkages).[26] Notably, all previously disclosed examples involve complex precursors, tediously synthesized and structurally incompatible with our aim, *i.e.* the scalable production to renewable chemical building blocks from cheap, bioderived platform molecules.

Results and discussion

Precursor design and reaction optimization

Promisingly, a small variation on the initial acrylate attempt already showed some DA cycloaddition activity: the furfuryl allyl ether **2a** gave some of the corresponding adduct **3a** (neat, 80 °C, 24 h), albeit in a low isolated yield of 11% and low chemoselectivity (33%) (Scheme 1). While modest, this activity did suggest that enhancing the population of the reactive conformer is a more important contributor to the feasibility of the reaction than activation of the olefin by an electron-withdrawing substituent is. Accordingly, we shifted focus to diallyl acetal **2b**, a furfural derivative, which we anticipated to be a superior DA substrate due to enhanced conformational flexi-
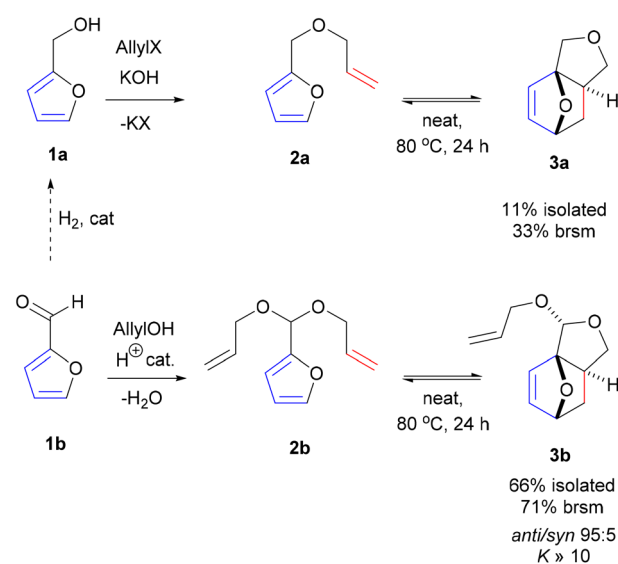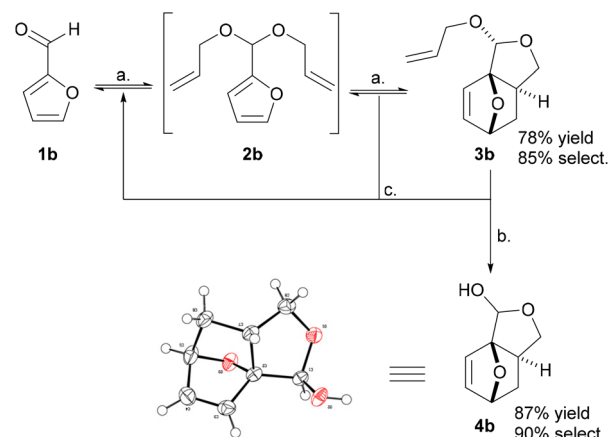

Scheme 1 Intramolecular DA cycloadditions with furfural allyl ether **2a**/furfural diallyl acetal **2b**; brsm = based on recovered starting material.

bility, favorable statistics and potentially the Thorpe–Ingold effect; moreover, the direct use of **2b** is highly desirable from a redox-economy point of view. Gratifyingly, the formation of **3b** under similar conditions turned out to be significantly more exergonic ($K \approx 10$ *vs.* $K < 1$ for **3a**); in addition, furfural **1b** and acetal **2b** are less prone to degradation as compared to **1a** and **2a**. Together, this allowed for the isolation of the adduct in a much-improved yield (66%) and selectivity.

With the intention to simplify the process as much as possible, we performed the acetalization and the cycloaddition in one single step. Thus, with excess allyl alcohol (10 equiv.), catalytic trifluoroacetic acid (TFA) (10 mol%) and in the presence of 3 Å molecular sieves, both the acetalization and the cycloaddition equilibria are pushed towards **3b**, which was produced in 75–80% yield after 24 h at 100 °C. The reaction was 100% *exo*-stereoselective due to the high preference for *cis* disposition of the fused C5–C6 rings; the diastereoisomeric ratio of the resulting *anti*- and *syn*-acetal pair was also very high, at ~95 : 5. Monitoring the reaction in time showed the transformation to be selective, both at low as well as high furfural conversions (Fig. 2) and to be near to equilibrium after 24 h. Note that the DA reaction proceeds with thermal activation alone and TFA does not play a catalytic role here in this reaction. Indeed, furfural diallyl acetal conversion to the DA adduct in the absence of TFA was comparable.

While **3b** (oil at ambient temperature) can be separated from unconverted furfural and **2b** by chromatography (and presumably by vacuum distillation), we envisaged that a more convenient purification by crystallization would be possible after deprotection of the acetal group (which also offers the additional advantage of further valorization of the *combined* diastereoisomeric acetal pair). Acid hydrolysis of **3b** towards **4b** was facile (HCl 2 equiv., H$_2$O, 50 °C) and highly selective; **4b**, a crystalline solid (see Scheme 2 for the X-ray crystal structure) could be isolated in highly pure form by precipitation. While **4b** is exclusively *anti* in the solid state, in solution the hemiacetal diastereoisomeric structures are in a solvent-dependent equilibrium; this suggest that the open hydroxy-aldehyde form

Scheme 2 Selective one-pot furfural acetalization/DA cycloaddition/deprotection towards tricyclic hemiacetal **4b**; XRD structure of isolated solid *anti*-**4b**; note that in solution, the *anti* and *syn* hemiacetal forms are in a solvent-dependent equilibrium.

One-pot acetalization/cycloaddition/hydrolysis:
a. allyl alcohol (10 equiv, TFA 10 mol%, 3Å MS, 100 °C, 24 h)
b. HCl aq (2 equiv), 50 °C, 17 h
c. recycle of recovered **1b** (and allyl alcohol)

Total yield over 3 steps (from **1b**): 67% (77% selectivity)

(*i.e.* the formal adduct of furfural and ally alcohol), is accessible for chemical derivatization, see Scheme 3 below and the ESI for more details.†

Deprotection also converts residual **2b** to furfural, which can be recovered for recycling; similarly, (the excess) allyl alcohol can also be readily recovered at either stage of the synthesis by distillation. As there was no indication of side reactions involving allyl alcohol (according to GC and NMR analyses), this component can in principle be recovered in entirety; only one equivalent is incorporated in the final product **4b**.

This synthesis proved very robust and scale-up to >100 mmol was facile. The acetalization/DA reaction produced adduct **3b** in 78% yield, with 85% selectivity and the remainder almost fully accounted for with 6% unconverted **1b** and 8% residual **2b**. The acid hydrolysis of this crude reaction mixture proceeded with approx. 90% selectivity, and a very high isolated yield of the pure hemiacetal **4b** (87%).

Reaction scope

With this promising synthetic route in hand, the intramolecular DA cycloaddition of the acetals of other readily available biobased 5-substituted furfurals was studied (Table 1). Notably, under similar reaction conditions, the ratio of **3** : **2** (calculated by NMR analysis of the crude reaction mixtures) was in all examples around 10 or higher; this suggests that the thermodynamics of the reaction is not negatively impacted by the substitution at the furan 5-position. Exceptionally, for R = Br, this ratio is at least 19 : 1; this positive impact of a halogen substituent on the intramolecular furan DA, the 'halogen-effect',[27–29] has been observed before.
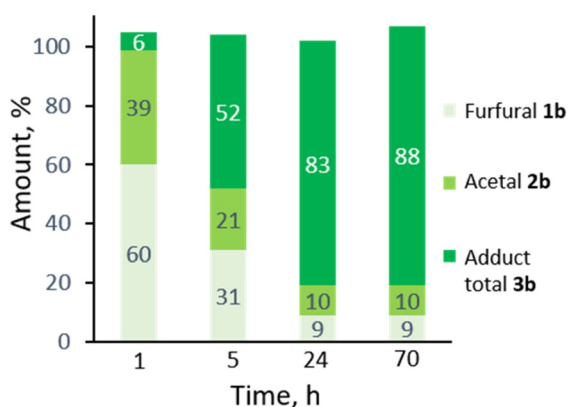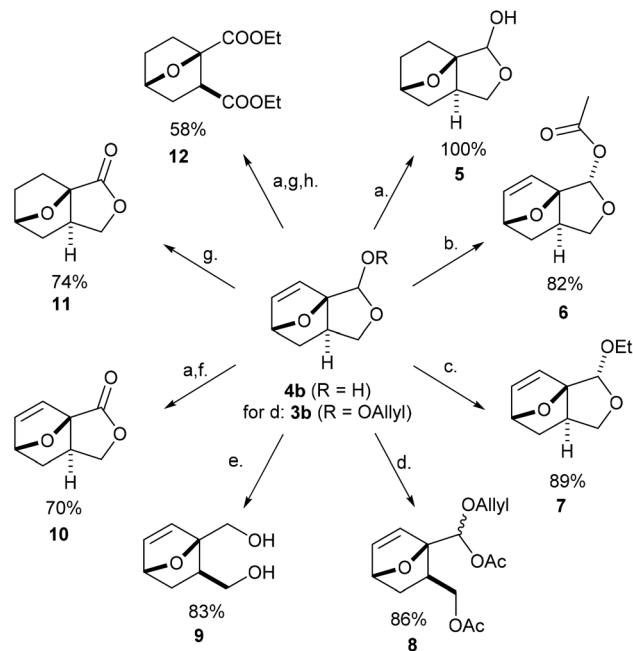

Fig. 2 Profile of the one-pot acetalization/DA in time (20 equiv. allyl alcohol, TFA 10 mol%, 3 Å MS, 100 °C).

Scheme 3 Functionalization of the novel DA adducts into value-added products; unless otherwise stated, **4b** is the starting point: (a) Pd/C (0.5 wt%), H₂, EtOAc, rt, 22 h; (b) AcCl, TEA, DCM, rt, 5 h; (c) Amberlyst-H cat., EtOH, 30 °C, 20 h; (d) MeSO₃H, Ac₂O, 50 °C, 2 h, using **3b** as starting material (R = Allyl); (e) NaBH₄, MeOH, rt, 2 h; (f) CuBr (5 mol%), TEMPO (5 mol%), bipy, NMI, MeCN, rt, 2 d; (g) Shvo's cat. (0.05 mol%), acetone, 50 °C, 4 d; (h) (1) EtOH, HCl, rt, 21 h; (2) NaClO₂, NaClO, TEMPO cat., rt, 48 h, (3) SOCl₂, EtOH, rt, 21 h.

Table 1 Furan scope of the one-pot acetalization/DA sequence
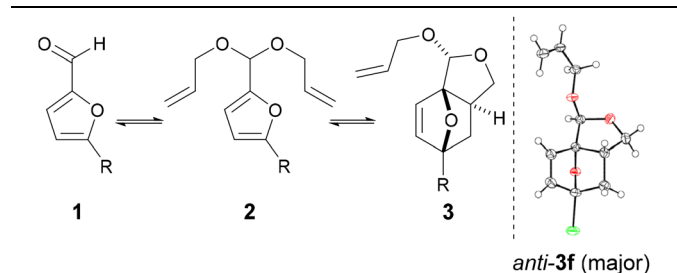
| Entry	R	Furan	**1**, %	**2**, %	Yield **3**, %	*dr* **3**, *anti* : *syn*
1	H	**1b**	8%	7%	69% (53%)	96 : 4
2	Me	**1c**	26%	5%	54% (41%)	95 : 5
3	CH₂OH	**1d**	22%	5%	47% (31%)	96 : 4
4	CH₂OEt	**1e**	11%	6%	72% (60%)	93 : 7
5	Br	**1f**	7%	<4%	76% (56%)[a]	83 : 17

General procedure: **1** and allyl alcohol (10 equiv.), TFA (10 mol%), 3 Å MS, 100 °C, 24 h; residual **1** and **2**, yield of **3** and dr of **3** refer to crude values determined by quantitative ¹H-NMR analysis; isolated yields of purified *anti*-**3** in brackets. [a] 12% of *syn*-**3f** also isolated.

This reaction was somewhat less diastereoselective, however, with a ratio of *anti*-**3f** to *syn*-**3f** of 83 : 17. For all the other examples, the minor *syn*-**3** diastereoisomer accounted for ≤7%; resolution of the diastereoisomers was in all cases possible by chromatography. Notably, single crystal X-ray structure determination of the major **3f** isomer allowed the unambiguous assignment of the configuration of the acetal centers in the series (Table 1). In terms of the reaction's overall performance, adducts **3e** (R = CH₂OEt) and **3f** (R = Br) were obtained in comparable yields to the title example **3b**, whereas for R = Me and R = CH₂OH the less efficient acetalization of **1** limited the yields to somewhat lower values.

Follow-up chemistry

With easy access to gram quantities of **4b**, we explored the synthetic potential of this novel DA adduct. The scaffold proved highly versatile and selective functionalization of the unsaturated hemiacetal into various added-value products was facile, as summarized in Scheme 3. Catalytic hydrogenation of the olefinic bond proceeded quantitatively on Pd/C, without compromising the reduction-labile hemiacetal group; this conversion is important in preventing side reactions resulting from the retro-DA channel (at temperatures >70 °C and/or in the presence of activators).[30,31] Next, the free OH group underwent facile ester- and etherification, giving **6** and **7** in high yields under mild conditions (preserving the *anti*-stereochemistry). These fragrant molecules show structural similarities to aroma compounds like camphor and eucalyptol and might accordingly find use in the fragrances industry. Ensuing, the masked aldehyde functionality in **4b** (or **3b**) can be exploited in producing carbonyl derivatives upon the opening of the fused C5 ring, for instance the α-allyloxyalkyl acetate **8** (by treatment of **3b** with MeSO₃H in Ac₂O) and oxime **13** (see Scheme 4). Alternatively, the hemiacetal ring can also be opened reductively with NaBH₄, leading to diol **9**, a bifunctional compound
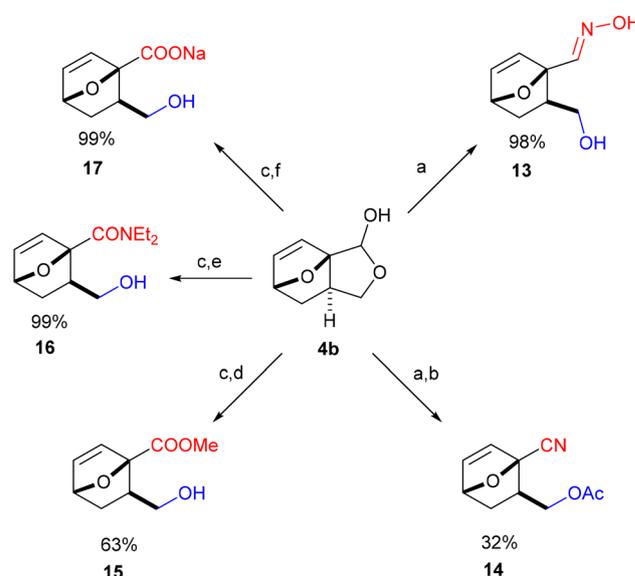
Scheme 4 Divergent access of atypical furan DA adducts starting from platform molecule **4b**: (a) NH₂OH·HCl, NaHCO₃, water, rt, 17 h; (b) DMAP (10 mol%), Ac₂O, NEt₃, CH₂Cl₂, rt, 6 d; (c) CuBr (5 mol%), TEMPO (5 mol%), bipy, NMI, MeCN, rt, 2 d; (d) AmberlystH, MeOH, rt, 2 h; (e) Et₂NH, rt, 18 h; (f) NaOH, MeOH, rt.

with potential use in polymer applications. Otherwise, going up the oxidation scale can be performed aerobically with the Cu/TEMPO catalytic system, producing the unsaturated tricyclic lactone **10**;[32] oxidation by transfer hydrogenation failed on **4b** but proved feasible with **5** as substrate (with Shvo's catalyst), affording the saturated analogue **11** in 74% isolated yield. This lactone served as precursor for the straightforward synthesis of diester **12**, a molecular analogue of diethyl *o*-phthalate, and thus a potential bioderived functional replacement of this industrially-important chemical commodity. Thus, this novel furan DA platform allows straightforward access to arene analogues and, more generally, to highly functional molecular scaffolds endowed with reactivity for various applications, such as cross-linking agents, polyesters/urethanes, plasticizers, *etc*. Preliminary studies show that **4b** (and **3b**) are reluctant to aromatization under standard conditions (*e.g.* with MeSO$_3$H/Ac$_2$O), something which requires further study.

Finally, by simple functional group interconversion, key products **4b** and **10** can be elaborated into a variety of atypical oxanorbornenes, such as oxime **13**, nitrile **14**, ester **15**, amide **16** and carboxylate salt **17** (Scheme 4). Notably, together with many of the molecules in Scheme 3, these products are formally DA adducts of allyl alcohol, a dienophile that is not reactive enough to undergo direct cycloaddition reactions with furan and even less so with deactivated derivatives such as furfural (oxime), 2-furonitrile or methyl 2-furoate, as required here. Thus, our methodology is ideal for the rapid, efficient and divergent synthesis of (electronically-) unusual furan DA adducts, populating previously unexplored areas of the oxanorbornene chemical space (see also Fig. 1). In addition, this synthetic strategy allows for complete control over the regio- and (relative) stereochemistry of the products, which is an important advantage over other (DA-based) routes. In this respect, the *ortho*/*exo* configuration obtained here is most challenging, as it is severely disfavored sterically.[25]

Reaction mechanism

DFT calculations allowed for a better understanding of the factors contributing to the success of this reaction (B3LYP/6-311+g(d), GD3BJ dispersion, in methanol (SMD)) (Fig. 3). In accordance with experiment, *anti*-**3b** was found to be more stable than *syn*-**3b** (by approx. 3 kcal mol^{-1}); only the pathway leading to the major isomer was investigated. As hypothesized and in contrast to furfuryl acrylate, the difference between the reactive conformation and the ground state is small for both furfuryl allyl ether **2a** and furfuryl diallyl acetal **2b**, 1.3 and 1.1 kcal mol^{-1}, respectively. This leads to thermally accessible kinetic barriers for the cycloaddition of 27.3 and 25.9 kcal mol^{-1}, respectively, in good agreement with the experimental observations (reactions proceed at 80–100 °C). Importantly, the cycloaddition with **2b** is confirmed to be significantly more exergonic (by approx. 3 kcal mol^{-1}) than the reaction with furfuryl allyl ether **2a**. This difference is indeed reflected in the experiments: in the studied temperature range (80–100 °C), the equilibrium was on the adduct side in the case of the acetal ($K \approx 10$) whereas the reaction with the ether was endergonic.
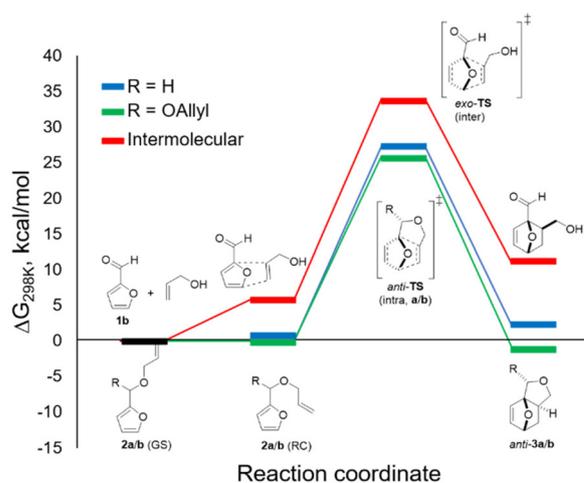

Fig. 3 DFT mechanism (calculated with B3LYP at 6-311+g(d) and GD3BJ dispersion, in methanol (SMD)); only the paths leading to the *anti*-**3** adducts were calculated; blue = furfuryl allyl ether **2a**; green: furfural diallyl acetal **2b**; red: intermolecular reaction between furfural and allyl alcohol; GS = ground state, RC = reactive conformation.

Finally, the DFT study allows us to rule out the intermolecular pathway: the direct cycloaddition between furfural and allyl alcohol is both considerably slower and endergonic relative to its intramolecular equivalent, as expected for this electronically-mismatched pair of addends. The strategy reported here thus provides a welcome alternative to still formally obtain the attractive, renewable adducts of this combination.

Conclusions

The remarkably selective furan Diels–Alder cycloaddition of furfural allyl acetals provides ready access to a highly versatile molecular scaffold and thus to a range of renewable chemical building blocks. Contrary to many related (intermolecular) [4 + 2] cycloadditions, the cyclization of furfural diallyl acetal is both kinetically and thermodynamically feasible at convenient operating temperatures (80–100 °C). Importantly, the route provides straightforward access to various atypical furan adducts that are not accessible *via* the intermolecular coupling of the unreactive DA precursors (*i.e.* furfural and allyl alcohol). The high selectivity (including regio- and stereo-), operational simplicity and facile product purification allow for a scalable synthesis; in addition, the renewable origin of the two precursors and full carbon retention in the product, combined with the straightforward diversification of the tricyclic scaffold *via* atom-economical transformations make this chemistry highly attractive for the sustainable preparation of bioderived chemical products, both drop-in and new. Finally, given the high synthetic utility of furan DA reactions and the versatility of our novel adduct platform, we strongly believe this chemistry can also find application in other fields, such as drug discovery, artificial flavor development, and natural product synthesis.

Author contributions

R. C. C. and P. C. A. B. conceived the research, and directed and supervised the project. R. C. C. and E. H. designed and executed the experiments and analysed the data. M. L. performed the single crystal structure determination. R. C. C. and P. C. A. B. acquired funding for the project. R. C. C., E. H. and P. C. A. B. wrote the paper and all authors commented on different versions of the manuscript.

Conflicts of interest

There are no conflicts to declare.

Acknowledgements

References

1 F. A. Kucherov, L. V. Romashov, G. M. Averochkin and V. P. Ananikov, *ACS Sustainable Chem. Eng.*, 2021, **9**, 3011–3042.

2 P. Vogel, J. Cossy, J. Plumet and O. Arjona, *Tetrahedron*, 1999, **55**, 13521–13642.

3 S. Roscales and J. Plumet, *Heterocycles*, 2015, **90**, 741–810.

4 S. Bur and A. Padwa, in *Methods and Applications of Cycloaddition Reactions in Organic Syntheses*, ed. N. Nishiwaki, John Wiley & Sons, Inc, 1st edn, 2014, pp. 355–406.

5 C. E. Puerto Galvis, L. Y. Vargas Méndez and V. V. Kouznetsov, *Chem. Biol. Drug Des.*, 2013, **82**, 477–499.

6 M. Gregoritza and F. P. Brandl, *Eur. J. Pharm. Biopharm.*, 2015, **97**, 438–453.

7 T. Elschner, F. Obst and T. Heinze, *Macromol. Biosci.*, 2018, **18**, 1800258.

8 H. Sun, C. P. Kabb, M. B. Sims and B. S. Sumerlin, *Prog. Polym. Sci.*, 2019, **89**, 61–75.

9 M. Vauthier, L. Jierry, J. C. Oliveira, L. Hassouna, V. Roucoules and F. B. Gall, *Adv. Funct. Mater.*, 2019, **1806765**, 1–16.

10 Y.-L. Liu and T.-W. Chuo, *Polym. Chem.*, 2013, **4**, 2194–2205.

11 A. E. Settle, L. Berstis, N. A. Rorrer, Y. Roman-Leshkóv, G. T. Beckham, R. M. Richards and D. R. Vardon, *Green Chem.*, 2017, **19**, 3468–3492.

12 R. F. A. Gomes and J. M. J. M. Ravasco, *ChemSusChem*, 2021, **14**, 3047–3053.

13 A. Maneffa, P. Priecel and J. A. Lopez-Sanchez, *ChemSusChem*, 2016, **9**, 2736–2748.

14 S. Dutta and N. S. Bhat, *Biomass Convers. Biorefin.*, 2023, **13**, 541–554.

15 H. Zhang, M. Jiang, Y. Wu, L. Li, Z. Wang, R. Wang and G. Zhou, *Green Chem.*, 2021, **23**, 2437–2448.

16 H. Zhang, M. Jiang, Y. Wu, L. Li, Z. Wang, R. Wang and G. Zhou, *ACS Sustainable Chem. Eng.*, 2021, **9**, 6799–6809.

17 C. Plass, N. Adebar, R. Hiessl, J. Kleber, A. Grimm, A. Langsch, R. Otter, A. Liese and H. Gröger, *Eur. J. Org. Chem.*, 2021, 6086–6096.

18 R. C. Cioc, M. Lutz, E. A. Pidko, M. Crockatt, J. C. van der Waal and P. C. A. Bruijnincx, *Green Chem.*, 2021, **23**, 367–373.

19 I. Scodeller, S. Mansouri, D. Morvan, E. Muller, K. De Oliveira Vigier, R. Wischert and F. Jérôme, *Angew. Chem., Int. Ed.*, 2018, **57**, 10510–10514.

20 F. A. Kucherov, K. I. Galkin, E. G. Gordeev and V. P. Ananikov, *Green Chem.*, 2017, **19**, 4858–4864.

21 G. Averochkin, E. Gordeev, M. Skorobogatko, F. Kucherov and V. P. Ananikov, *ChemSusChem*, 2021, **14**, 3110–3123.

22 J. Iglesias, I. Martínez-Salazar, P. Maireles-Torres, D. Martin Alonso, R. Mariscal and M. López Granados, *Chem. Soc. Rev.*, 2020, **49**, 5704–5771.

23 R. C. Cioc, T. J. Smak, M. Crockatt, J. C. van der Waal and P. C. A. Bruijnincx, *Green Chem.*, 2021, **23**, 5503–5510.

24 K. I. Galkin and V. P. Ananikov, *Int. J. Mol. Sci.*, 2021, **22**, 11856.

25 C. S. Lancefield, B. Fölker, R. C. Cioc, K. Stanciakova, R. E. Bulo, M. Lutz, M. Crockatt and P. C. A. Bruijnincx, *Angew. Chem., Int. Ed.*, 2020, **59**, 23480–23484.

26 F. Lewis and L. Harwood, in *Targets in Heterocyclic Systems*, 2012, pp. 1–30.

27 S. N. Pieniazek and K. N. Houk, *Angew. Chem., Int. Ed.*, 2006, **45**, 1442–1445.

28 R. L. Rae, J. M. Zurek, M. J. Paterson and M. W. P. Bebbington, *Org. Biomol. Chem.*, 2013, **11**, 7946–7952.

29 A. Padwa, K. R. Crawford, C. S. Straub, S. N. Pieniazek and K. N. Houk, *J. Org. Chem.*, 2006, **71**, 5432–5439.

30 S. Thiyagarajan, H. C. Genuino, M. Śliwa, J. C. Van Der Waal, E. De Jong, J. Van Haveren, B. M. Weckhuysen, P. C. A. Bruijnincx and D. S. Van Es, *ChemSusChem*, 2015, **8**, 3052–3056.

31 S. Thiyagarajan, H. C. Genuino, J. C. Van Der Waal, E. De Jong, B. M. Weckhuysen, J. Van Haveren, P. C. A. Bruijnincx and D. S. Van Es, *Angew. Chem., Int. Ed.*, 2016, **55**, 1368–1371.

32 J. M. Hoover, J. E. Steves and S. S. Stahl, *Nat. Protoc.*, 2012, **7**, 1161–1166.